International Journal of Minerals, Metallurgy and Materials
Volume 22, Number 2, February 2015, Page 210
DOI: 10.1007/s12613-015-1063-5

Fabrication method and microstructural characteristics of coal-tar-pitch-based 2D carbon/carbon composites

Mohammad Esmaeeli[1)], *Hamed Khosravi*[2)], *and Alireza Mirhabibi*[1)]

1) School of Metallurgy and Materials Engineering, Iran University of Science and Technology, Tehran 13114-16846, Iran
2) Faculty of Materials Science and Engineering, K. N. Toosi University of Technology, Tehran 19991-43344, Iran
(Received: 12 May 2014; revised: 30 May 2014; accepted: 4 June 2014)

Abstract: The lignin-cellulosic texture of wood was used to produce two-dimensional (2D) carbon/carbon (C/C) composites using coal tar pitch. Ash content tests were conducted to select two samples among the different kinds of woods present in Iran, including walnut, white poplar, cherry, willow, buttonwood, apricots, berry, and blue wood. Walnut and white poplar with ash contents of 1.994wt% and 0.351wt%, respectively, were selected. The behavior of these woods during pyrolysis was investigated by differential thermal analysis (DTA) and thermo gravimetric (TG) analysis. The bulk density and open porosity were measured after carbonization and densification. The microstructural characteristics of samples were investigated by scanning electron microscopy (SEM), X-ray diffraction (XRD), and Fourier-transform infrared (FT-IR) spectroscopy. The results indicate that the density of both the walnut and white poplar is increased, and the open porosity is decreased with the increasing number of carbonization cycles. The XRD patterns of the wood charcoal change gradually with increasing pyrolysis temperature, possibly as a result of the ultra-structural changes in the charcoal or the presence of carbonized coal tar pitch in the composite's body.

Keywords: carbon/carbon composites; microstructure; porosity; density; densification; carbonization

1. Introduction

As a result of hundreds of millions of years of heredity and evolution, natural species develop into rational microstructures. Recently, materials synthesized through biological structures have attracted particular interest [1–2]. The shape, size, and distribution of components in metal or ceramic matrix composites generally depend on fabrication processes. However, the technique of fabricating materials with desired and delicate microstructures is still not simple. Wood can be considered as a natural composite material with a hierarchical architecture, where the cellulose and lignin form the cellular microstructures [3]. When wood is heated at high temperature for carbonization, mixed biopolymers in wood are decomposed into carbon and gases. This decomposition gives rise to a porous carbon with a morphology derived from its wood template. The porosity and surface area play great roles in the combustion of wood [4–5].

The porous carbon has many favorable characteristics, such as low coefficient of thermal expansion, low and stable friction coefficient, high directional stiffness, low density, high special strength, good electromagnetic shielding properties, and high damping capacity [1–2]. These characteristics mean that the porous carbon can be used in several industrial fields to improve the performance of many new products, such as activated carbons, pyrolytic carbon deposited in wood char, lignocellulose/pitch-based composites, cellular ceramics, duplex Si/SiC ceramic composites based on wood templates, C/polymer materials, and different kinds of C/C composites [6–12]. In this study, a C/C composite was fabricated using a preform with a wood-like structure. The composite material was obtained by injecting the molten coal tar pitch under a specific pressure and temperature into the porous carbon derived from wood. This approach was used to increase the density and improve the mechanical properties of C-templates.

Corresponding author: Hamed Khosravi E-mail: hkhosravi@mail.kntu.ac.ir

2. Experiments

The ash content of eight different kinds of Iranian wood (walnut, white poplar, cherry, willow, button wood, apricots, berry, and blue wood) was analyzed according to the ASTM D3174 method. For the thermal analysis of wood powders (ASTM E.11, mesh No. 60), 2–3 mg of each species were studied using a Perkin-Elmer Diamond thermo gravimetric/differential thermal analyzer (PED TG/DTA). The samples were loaded into the unsealed alumina crucibles and were subsequently heated from room temperature to 1000°C at a rate of 10°C/min with a 200 mL/min purge rate. Nitrogen gas was used as the purge gas. The heating of selected woods was conducted in a steel mold with dimensions of 200 mm × 150 mm × 150 mm placed in the furnace. The samples were first pyrolyzed at 600°C for 2 h to produce the porous carbon. Then, the pyrolyzed woods were densified using molten coal tar pitch in seven impregnation/re-carbonization cycles.

Powdered $PA_{63}X$ coal tar pitch (ASTM E.11, mesh No. 30) was used as an impregnant; its specifications are shown in Table 1. Impregnation was performed in a stainless steel mold with dimensions of 500 mm × 150 mm × 150 mm. Eight specimens with dimensions of 100 mm × 30 mm × 30 mm for each type of wood were used. The mold was placed in an autoclave, and the temperature was increased to 250°C to decrease the viscosity of pitch. Nitrogen gas was subsequently injected at pressure of 3 MPa to facilitate the impregnation process. After each cycle, the samples were re-carbonized in the furnace. For the re-carbonization process, the heating rate and maximum temperature were 0.5 C/min and 1000°C, respectively.

Table 1. Specifications of $PA_{63}X$ coal tar pitch

Charring yield / %	Softening point / °C	Insoluble toluene / vol%	Density before carbonization / ($g \cdot cm^{-3}$)	Density after carbonization / ($g \cdot cm^{-3}$)
52	120–130	29	1.31	2.02

Scanning electron microscopy (SEM) was used to study the morphology and microstructure of the porous carbon and C/C composites. The bulk density and open porosity of the porous carbon and C/C composites were determined after each densification cycle according to the standard method of BS EN 993-1.

The structures of the obtained samples were characterized by X-ray diffraction (XRD) measurements using a Cu K_α radiation source operated at a voltage of 30 kV and a current of 20 mA. The infrared spectra of the porous carbon and C/C composites were obtained on a Fourier-transform infrared (FT-IR) spectrophotometer using attenuated total reflection; the sample chamber was maintained under a nitrogen atmosphere with a flow rate of 5 L/min.

3. Results and discussion

3.1. Results of ash content

The test results of ash content are shown in Table 2. According to the results in this table, walnut, which exhibits the highest ash content (1.994wt%), and white poplar, which exhibits the lowest ash content (0.351wt%), are selected for further study.

3.2. Differential thermal analysis (DTA) results

The wood samples were destroyed via two mechanisms. The first mechanism occurs at temperatures less than 573 K, where cellulose walls are destroyed via the breakage of internal chemical links, resulting in the formation of free radicals, carbonyl and hydroperoxide groups, carbon monoxide, carbon dioxide, and activated charcoal. Oxidation of activated charcoal and secondary oxidation of flammable volatile gasses lead to non-flash and flash ignition, in order [13–14]. The second mechanism occurs at temperatures greater than 573 K and leads to the formation of secondary links and intermediate compounds such as polysaccharides and carbonized compounds. The DTA curves of the walnut and white poplar are shown in Fig. 1.

Table 2. Ash content of different woods wt%

White poplar	Apricots	Willow	Cherry	Blue wood	Button-wood	Berry	Walnut
0.351	0.558	0.612	0.702	1.109	1.154	1.811	1.994

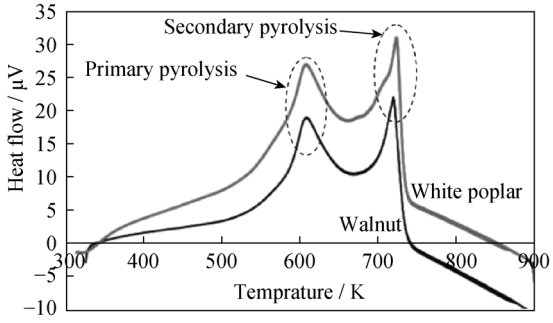

Fig. 1. DTA curves of the walnut and white poplar.

When the woods were pyrolyzed, two exothermic peaks were identified at 603 and 723 K during the process. The first peak was associated with the wood combustion and the removal of carbon monoxide, methane, formaldehyde, acetic acid, formic acid, methanol, hydrogen, and flammable tars. The second peak was related to the combustion of the remaining charcoal and flammable gases during the secondary pyrolysis stage [13,15].

3.3. Thermo gravimetric (TG) analysis

The weight loss of the pyrolyzed woods was evaluated in the present study. The water present in the woods was volatilized before the beginning of thermal decomposition of the wood constituents [15–16]. As shown in Fig. 2, the weights of samples (i.e., walnut and white poplar) decrease with increasing charring temperature, and the curve gradually decreases with a gentle slope until it stabilizes at approximately 520 K. A sharp increase in sample weight occurs at temperatures above 520 K. These significant weight losses may originate from the pyrolysis of principal chemical constituents — cellulose, hemicelluloses, and lignin — in the cell walls. Hemi-celluloses decompose at temperatures between 473 and 573 K, followed by the cellulose decomposition above 513 K and lignin above 553 K [13]. At 600 K, the weight loss curves are less steep than those associated with the previous losses; then the curves stabilize above 723 K. These losses are attributable to the removal of volatile materials and to the evaporation of attracted moisture. High weight losses of samples are caused by the activated pyrolysis and the production of flammable gasses, such as carbon monoxide, methane, formaldehyde, acetic acid, formic acid, methanol, hydrogen, and flammable tars [14].

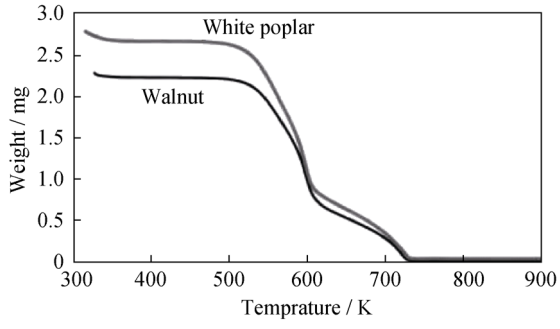

Fig. 2. Weight loss curves of the walnut and white poplar.

3.4. Evaluation of impregnation process

Densification efficiency is a function of the following parameters: (a) the inherent properties of samples, such as the initial density, the distribution, shape, depth, and size of pores (or vessel), and the connection mode of pores to the surface; (b) the properties and behavior of the impregnant, such as the viscosity of the molten metal, softening point, charring yield, and density before and after the carbonization process; and (c) the impregnation conditions, such as the temperature, pressure, and time of impregnation. In general, large pores, voids, and cracks or ruptures in the samples investigated in this work are easily impregnable. According to thermodynamics, the presence of microspores is not advantageous, because, in this case, the surface energy increases with the infiltration of the precursor into the pore [17]. The impregnation rate is defined as the increment of the matrix precursor in the unit volume per time (dV/dt) of the composite, which is equivalent to the definition of the volume flow rate in physical chemistry. Its precise mathematical expression can be derived only for the model pores with a defined size and shape. In the case of cylindrical pores and a precursor that exhibits Newtonian behavior, it can be written as the following equation [17]:

$$\frac{dV}{dt} = \frac{\pi R^4 \Delta P}{8\eta L} \tag{1}$$

where R is the pore radius, ΔP the driving force, η the viscosity, and L the pore length. From this equation, the dominant influence of the pore radius on the impregnation rate is evident. Also, the impregnation rate increases with an increase in external pressure or a decrease in the impregnant viscosity and pore length. The SEM images obtained for the impregnated C-template in the section vertical to fibers are shown in Fig. 3. However, in this view, the depth of impregnation is not observable. According to Fig. 4, the lignocellulosic fibers do not fill. Also, the observed impregnation depth in vessels decreases with an increase in their length; in addition, three impregnation depths (full-impregnated, semi-impregnated, and non-impregnated) are observed in Fig. 4.

Non-saturated cellulosic fibers are affected by two factors: (1) the fiber diameter is not proportional to the applied pressure (i.e., 3 MPa); thus, it prevents the penetration of the molten pitch into the fibers' throats; and (2) the fibers are discontinuous because different membranes those actually absorb the nutrient filters are in their path. These filters inhibit the penetration of the molten pitch. This interpretation is completely revealed in the filters shown in Fig. 5. Unlike the hollow fibers, the vessels exhibit a much greater diameter and depth, and the molten pitch easily penetrates into them. However, greater impregnation requires vessels with a greater depth. In addition, because of the presence of residual carbon on their walls, these open porosities become closed porosities after the impregnation cycles [17].

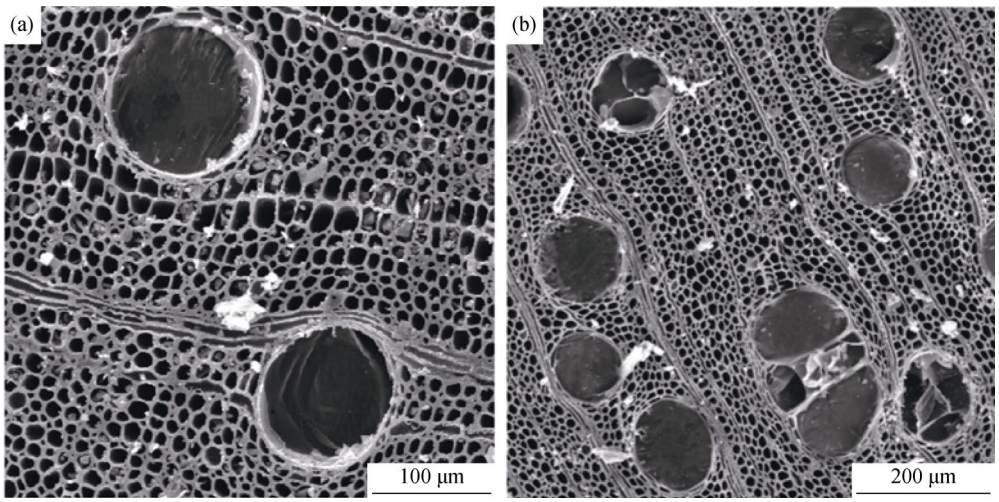

Fig. 3. Two different magnifications of SEM micrographs of the impregnated pyrolyzed samples.

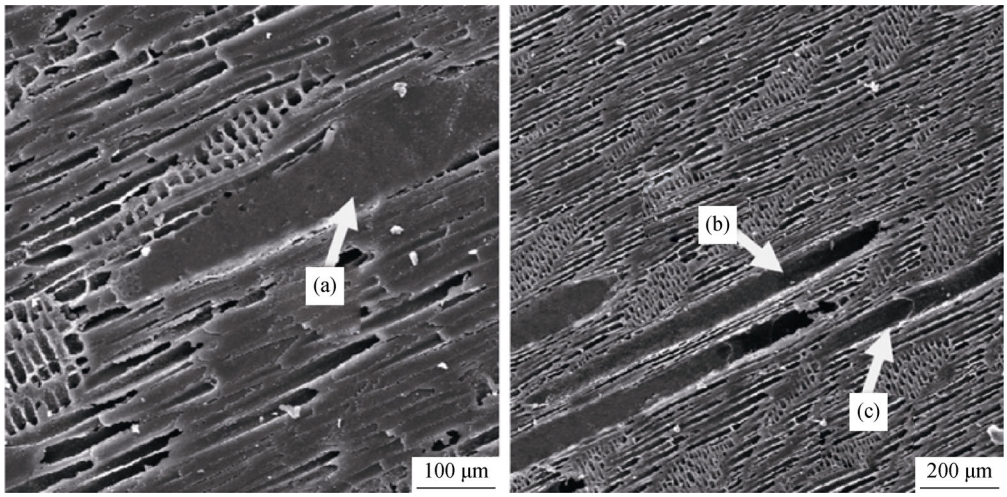

Fig. 4. SEM micrographs of the impregnated pyrolyzed wood: (a) full-Impregnated vessel; (b) semi-impregnated vessel; (c) non-impregnated vessel.

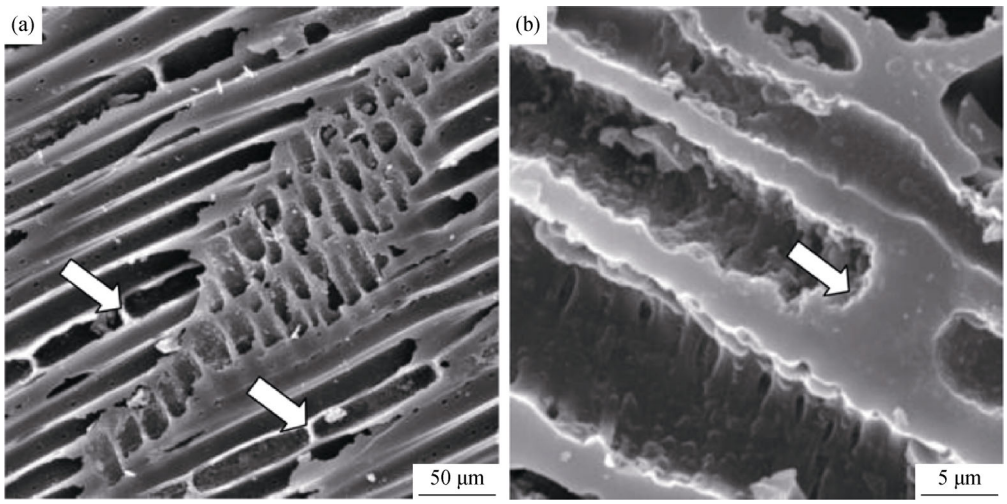

Fig. 5. SEM micrographs of the impregnated pyrolyzed wood and the absorbing nutrient filters of fibers.

3.5. Densification efficiency

The bulk density and open porosity content of samples before and after each densification cycle were estimated according to the standard method BS EN 993-1. The measured values are presented in Fig. 6. In term of curves, the results indicate an increase in the bulk density from 1.051 g/cm^3 to 1.421 g/cm^3 for the walnut composite and from 0.66 g/cm^3 to 1.022 g/cm^3 for the white poplar composite after seven cycles of densification. The results also indicate a decrease in the open porosity from 34.57% to 13.22% for the walnut composite and from 50.75% to 28.21% for the white poplar composite.

The volumetric densification efficiency (y_v), as defined in Eq. (2), was calculated from the open porosity and bulk density data as follows [18].

$$y_v(n) = \frac{\rho_b(n) - \rho_b(n-1)}{\theta(n-1)\cdot\rho_c} \quad (2)$$

where $y_v(n)$ is the volumetric densification efficiency of the nth densification cycle, $\rho_b(n)$ the bulk density after the nth densification cycle, $\theta(n)$ the open porosity after the nth densification cycle, and ρ_c the density of the decarbonized pitch. The evolution of the calculated densification efficiency with the number of densification cycles is presented in Fig. 7. In general, the densification efficiency exhibits an inverse trend with respect to the number of densification cycles, as clearly indicated in Fig. 7.

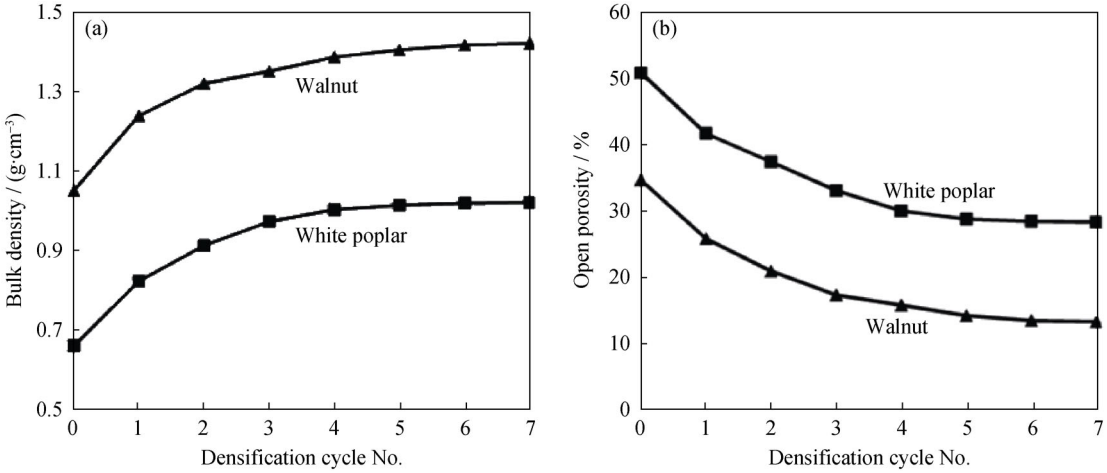

Fig. 6. Bulk density (a) and open porosity content (b) of the C/C composites in terms of the number of densification cycles.

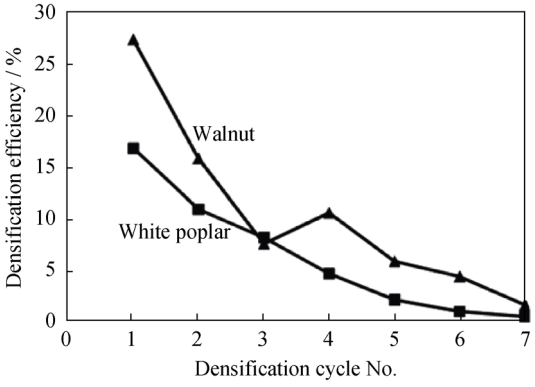

Fig. 7. Densification efficiency of the C/C composites as a function of the number of densification cycles

3.6. X-ray diffraction (XRD)

The XRD patterns of the wood charcoal and C/C composite before and after seven cycles of impregnation/carbonization for both the walnut and white poplar composites are shown in Fig. 8. The figures indicate sharp peaks in the approximate 2θ range of 15°–30°; these peaks are related to the presence of cellulose and some lignin or hemi-celluloses. After the samples were carbonized at 600°C, the peaks gradually became weak and broad. For the two kinds of wood charcoal shown in Figs. 4(a) and 5(a), two weak and broad diffraction peaks were observed, reflecting the low crystallinity of carbon obtained from the carbonization of cellulose [19].

As shown in Figs. 4(b) and 5(b), after seven impregnation/carbonization cycles at 1000°C, two diffraction peaks were detected, which were more intense than those of the wood charcoal. These results proved that the amount of crystallized carbon obtained from carbonized woods could be increased at elevated temperatures [4]. Nishimiya *et al.* [19] showed that the XRD patterns of the wood charcoal changed gradually with increasing temperature, possibly because of the ultrastructure changes in charcoal. Therefore, the sharp peaks appeared to originate from the crystalline graphite structure that appeared in charcoal carbonized at 1800 and 2000°C. These results suggested that the wood charcoal and C/C composite were not composed of completely graphitized carbon structures but had a turbostratic

structure [17,20]. Also, after seven cycles of densification, the molten coal tar pitch was impregnated into the porous charcoal and remained in the wood's vessels after carbonization. Among the different impregnants, the coal tar pitch exhibited by far the greatest crystallinity. Our observation of two fairly sharp and narrow peaks in the XRD patterns of samples was attributable to the presence of carbonized coal tar pitch in the composite's body [21].

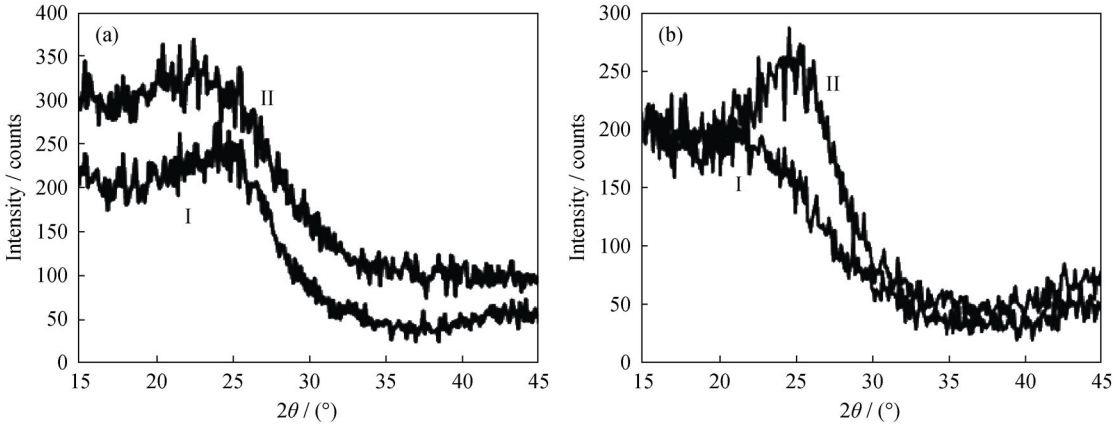

Fig. 8. XRD patterns of the walnut (a) and white poplar wood (b): (I) before densification; (II) after seven cycles of densification.

3.7. FT-IR spectroscopy

Fig. 9 shows the FT-IR spectra of the C/C composite after 2, 4, and 7 cycles of densification (impregnation/carbonization) for two kinds of Iranian woods. The infrared spectra of products were not clearly resolved because of the greater absorbance of visible light rays by wood charcoal as a consequence of its black color. As evident in the spectra in Fig. 9, the C–H deformation vibration mode (approximately 1400 cm^{-1}) and the O–N=O mode (approximately 2000–2200 cm^{-1}) were weakly detected. Also, the C=C aromatic mode (approximately 1600 cm^{-1}) and the C–O mode (approximately 1500 cm^{-1}) were clearly detected. These modes increased in intensity with further densification, especially in the case of walnut because of the substantially greater cellulose and lignin contents. As a result, the decomposition of volatile gasses, such as H_2O, CO, and CO_2, and the formation of pyranose rings proceeded with an increase in the number of densification cycles. It was assumed that the temporary formation of the C–O and C=C modes was caused by the formation of H_2O in a pyranose ring during the primary carbonization step, because these modes did not exist in the original cellulose. A large and broad band was observed at approximately 1400–1700 cm^{-1}. This band was assigned to the presence of lignin in the wood charcoals. These results therefore suggested that the absorbance increased with the increased lignin content in the original woods. In this investigation, the walnut wood was observed to have a lignin content greater than that of the white poplar.

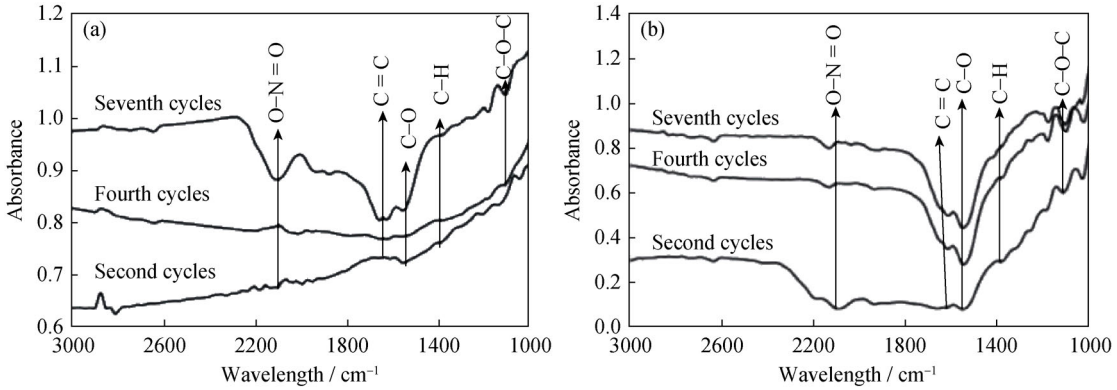

Fig. 9. FT-IR spectra of the C/C composites from the walnut (a) and white poplar wood (b).

4. Conclusions

(1) The lignin-cellulosic texture of wood is used to produce 2D C/C composites.

(2) An effective method for the production of preforms with sufficient strength to be carbonized and infiltrated was developed.

(3) The bulk density tends to increase with the increasing

number of densification cycles, which means that, for both the walnut and white poplar, the density increases, and the open porosity content decreases. The density of the walnut wood increases from 1.051 g/cm^3 to 1.421 g/cm^3 and its open porosity decreases from 34.57% to 13.22% during the densification cycles.

(4) The XRD patterns of the wood charcoal gradually change with increasing temperature, possibly because of the ultrastructural changes in the charcoal or because of the presence of carbonized coal tar pitch in the composite's body.

References

[1] T. Manabe, M. Ohata, S. Yoshizawa, D. Nakajima, S. Goto, K. Uchida, and H. Yajima, Effect of carbonization temperature on the physicochemical structure of wood charcoal, *Trans. Mater. Res. Soc. Jpn.*, 32(2007), No. 4, p. 1035.

[2] T.C. Wang, T.X. Fan, D. Zhang, and G.D. Zhang, Fabrication and the wear behaviors of the carbon/aluminum composites based on wood templates, *Carbon*, 44(2006), No. 5, p. 900.

[3] T.C. Wang, T.X. Fan, D. Zhang, and G.D. Zhang, Fabrication, thermal expansions, and mechanical properties of carbon/aluminum composites based on wood templates, *J. Mater. Sci.*, 41(2006), No. 18, p. 6095.

[4] Y. Ohzawa, M. Mitani, J.L. Li, and T. Nakajima., Structures and electrochemical properties of pyrolytic carbon films infiltrated from gas phase into electro-conductive substrates derived from wood, *Mater. Sci. Eng. B*, 113(2004), No. 1, p. 91.

[5] I. Külaots, A. Hsu, and E.M. Suuberg, The role of porosity in char combustion, *Proc. Combust. Inst.*, 31(2007), No. 2, p. 1897.

[6] M. Kumar and R.C. Gupta, Influence of carbonization conditions on the pyrolytic carbon deposition in acacia and eucalyptus wood chars, *Energy Sources*, 19(1997), No. 3, p. 295.

[7] G.A. Zickler, T. Schöberl, and O. Paris, Mechanical properties of pyrolysed wood: a nanoindentation study, *Philos. Mag.*, 86(2006), p. 1373.

[8] P. Colombo, Conventional and novel processing methods for cellular ceramics, *Philos. Trans. R. Soc. A,* 364(2006), No. 1838, p. 109.

[9] V. Pancholi, D. Mallick, Ch. AppaRao, I. Samajdar, O.P. Chakrabarti, H.S. Maiti, and R. Majumdar, Microstructural characterization using orientation imaging microscopy of cellular Si/SiC ceramics synthesized by replication of Indian dicotyledonous plants, *J. Eur. Ceram. Soc.,* 27(2006), p. 367.

[10] P. Álvarez, C. Blanco, R. Santamaría, and M. Granda, Lignocellulose/pitch based composites, *Compos. Part A*, 36(2005), No. 5, p. 649.

[11] Y.S. Virgil'ev and I.P. Kalyagina, Carbon-carbon composite materials, *Inorg. Mater.*, 40(2004), No. 1, p. S33.

[12] J.N. Sahu, J. Acharya, and B.C. Meikap, Optimization of production conditions for activated carbons from Tamarind wood by zinc chloride using response surface methodology, *Bioresour. Technol.*, 101(2010), No. 6, p. 1974.

[13] S.M. Kwon, N.H. Kim, and D.S. Cha, An investigation on the transition characteristics of the wood cell walls during carbonization, *Wood Sci. Technol.*, 43(2009), No. 5-6, p. 487.

[14] F.C. Beall and H.W. Elckner, Thermal degradation of wood components: a review of the literature, *U.S.D.A. Forest Service Research Paper*, U.S. Department of Agriculture, Forest Products Laboratory, Madison, 1970, p. 130.

[15] W. Brostow, K.P. Menard, and N. Menard, Combustion properties of several species of wood, *Chem. Chem. Technol.*, 3(2009), No. 3, p. 173.

[16] S.X. Liu, S.R. Zhang, B.N. Li, and W.H. Zhu, Thermal testing methods in determination of characterization of charcoals, *J. For. Res.*, 11(2000), No. 1, p. 60.

[17] M. Klučáková, Analysis of relationship between properties and behaviour of materials used and impregnation conditions of carbon-carbon composites, *Acta Mater.*, 53(2005), No. 14, p. 3841.

[18] S.S. Tzeng and J.H. Pan, Densification of two-dimensional carbon/carbon composites by pitch impregnation, *Mater. Sci. Eng. A*, 316(2001), No. 1-2, p. 127.

[19] K. Nishimiya, T. Hata, Y. Imamura, and S. Ishihara, Analysis of chemical structure of wood charcoal by X-ray photoelectron spectroscopy, *J. Wood Sci.*, 44(1998), No. 1, p. 56.

[20] T. Hirose, T. Fujino, T.X. Fan, E. Hiroyuki, T. Okabe, and M. Yoshimura, Effect of carbonization temperature on the structural changes of woodceramics impregnated with liquefied wood, *Carbon*, 40(2002), p. 761.

[21] G.R. Devi and K.R. Rao, Carbon-carbon composites: an overview, *Defence Sci. J.*, 43(1993), No. 4, p. 369.